

Plasma Welding of Steel CPW 800

Abstract: The article is concerned with issues related to the plasma welding of steel CPW 800 using titanium and niobium microagents. Plasma welding tests involving sheets subjected to TMCP were performed with various linear energy values. Welded joints were subjected to macro and microscopic metallographic tests, hardness measurements (involving the base material, HAZ and weld) as well as tensile and bend tests. The strength of the welded joints obtained in the tests was greater than that of the base material; a slight increase in the hardness of joint area ensured its relatively high plasticity.

Keywords: plasma welding, CPW 800, metallographic tests, hardness measurements

DOI: [10.17729/ebis.2016.2/2](https://doi.org/10.17729/ebis.2016.2/2)

Introduction

Because of their excellent mechanical properties combined with plastic workability and relatively good weldability, modern steels referred to as AHSS (Advanced High-Strength Steels) are becoming increasingly popular among automotive concerns perceiving AHSS as valuable structural materials. Good mechanical properties enable the reduction of car kerb weight by decreasing cross-sections of structural elements without compromising or even improving the passive safety of passengers [1-4]. Advanced High-Strength Steels are characterised by a complex and multiphase microstructure providing the favourable combination of strength and plasticity. Among others, AHSS include CP steels (Complex Phase).

Due to their chemical composition and mechanical properties provided through heat or thermoplastic treatment, CP type steels are rated within the upper range of strength and within the medium range of plasticity among other

AHSS Advanced High-Strength Steels [2, 3, 5]. In addition to martensite and ferrite, the structure of CP steels contains small amounts of retained austenite in the bainitic matrix (Fig. 1). This steel is characterised by a fine-grained structure. A small difference in hardness between individual structural components is responsible for the good “local ductility” of CP type steels, particularly desirable when bending sheet edges and turning up flanges [6].

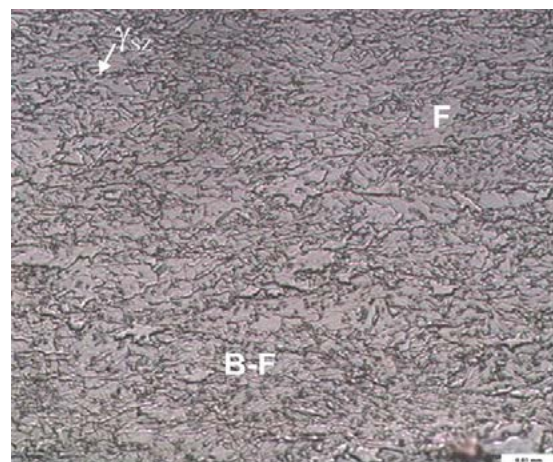


Fig. 1. Microstructure of steel CPW 800

For this reason, CP steels are used in the making of elements characterised by complicated shapes, e.g. side reinforcements of doors or elements of seat and floor panels [3, 6].

In addition to required mechanical properties, materials perceived by constructors and technologists as valuable and interesting must also be characterised by good workability in all technological processes accompanying the making of a finished product, i.e. pressing, welding, applying metallic coatings, painting etc.

Presently, because of high efficiency and reliability, the dominant technology used for joining car body elements is resistance welding [2, 7]. In addition, various laser welding methods and plasma welding are becoming increasingly popular as well.

The weldability of CP steels has rarely been addressed in scientific publications, with the majority of studies concerning laser welding [8]. Due to relatively low amounts of carbon in CP steels, their weldability should be relatively high. However, increased amounts of such chemical elements components as Cr, Mo, Si and/or Al increase the susceptibility to partial martensitic transformation. CP steels are distinguished by microagents used for grain refinement. In this aspect it is necessary to use experience related to joining HSLA steels made using the Thermo-Mechanical Control Process [9-11].

This article presents results of technological tests concerning the plasma welding of steel CPW 800, i.e. hot-rolled steel subjected to controlled cooling, manufactured by Thyssen-Krupp GmbH.

Test Material

The joints used in the tests were made of 2.5 mm thick steel CPW 800 (150 × 300 mm) cut out of sheets (1000 × 1500 mm) using a laser. The chemical composition of the sheet material, determined using spark source optical emission spectrometry and a Q4 TASMEN spectrometer manufactured by Bruker, is presented in Table 1.

Test Rig and Test Joints

The plasma tests were performed using a rig equipped with a Cloos-made Romat 310M welding robot, with a plasma torch affixed to its wrist. The plasma torch was an element of a Eutronic GAP 3001 plasma welding machine manufactured by Castolin (Fig. 2).



Fig. 2. Plasma welding station equipped with the Romat 310M welding robot manufactured by Cloos and the Eutronic GAP 3001 welding machine manufactured by Castolin

Before welding, an oxide layer was removed from cut edges, whereas the surface of the sheets (at a width of 50 mm from the welded edge) was degreased using acetone. Afterwards, the sheets were tacked at their ends using TIG welding by melting the edges of the

Table 1. Chemical composition and carbon equivalent C_e of steel CPW 800, % by weight according to check analysis

C	Mn	Si	Cr	S	P	Nb	Ti	N	Al	Mo	C_e
0.08	1.72	0.56	0.34	0.003	0.010	0.005	0.125	0.002	0.48	0.016	0.46

Note: carbon equivalent C_e was calculated according to the following formula:

$$C_e = C + \frac{Mn}{6} + \frac{Si}{24} + \frac{Ni}{40} + \frac{Cr}{5} + \frac{Mo}{4} [\%]$$

base material. The sheets were tacked without leaving a gap between them. Next, the tacked sheets were fixed in a manner preventing their movement during welding. The process of welding was performed on a copper pad. The plasma torch was provided with a tungsten electrode ($\phi 1.6$ mm) and a plasma nozzle (1.7 mm). The gas used both as shielding and plasma gas was argon. The flow of plasma gas was adjusted at 0.7 l/min, whereas that of shielding gas at 7 l/min. Current amounted to 63 A. The distance between the electrode and the material amounted to 5 mm. For the parameters mentioned above, the voltage of arc amounted to 28 V. Welding tests were performed at a welding rate of 22 cm/min and 33 cm/min. The calculated linear energy amounted to 0.48 kJ/mm and 0.32 kJ/mm respectively.

Tests and Results

Determining the effect of plasma welding on structural and mechanical changes of plasma welded joints required the performance of visual tests and destructive tests of the welded joints. The destructive tests involved macro and microscopic metallographic tests, cross-sectional hardness measurements of the joints, tensile tests and bend tests involving the extension of the face and root of the weld.

In the first place, the welded joints were subjected to visual tests. The joint made at a welding

rate of 22 cm/min revealed a 0.1 mm deep undercut on the weld face side. It should be noted that as regards joints having thicknesses of up to 3 mm, quality level B does not allow the presence of any undercuts. In turn, quality level C requires that the depth of an undercut must not exceed $0.1 t$, where t stands for the thickness of a material being welded. The faces and roots of welds made in technological tests are presented in Figure 3. After the visual tests, in order to determine the shape of the fusion line, the absence/presence of porosity and cracks in the weld and in the HAZ, it was necessary to perform macroscopic metallographic tests. Afterwards, in order to determine changes in the microstructure of the weld and in the HAZ, it was necessary to perform microscopic metallographic tests. The macroscopic metallographic tests were performed using an MeF4 light microscope manufactured by Leica. The macroscopic metallographic tests were performed at a magnification of 25x, whereas the microscopic metallographic tests were performed at a magnification of 500x. The microstructural tests involved the base material and the welded joint, i.e. the weld and the HAZ in two areas, i.e. in the area adjacent to the weld and on the base material side. The results of the macroscopic metallographic tests are presented in Figure 4; the microscopic metallographic test results are presented in Figures 5 and 6.

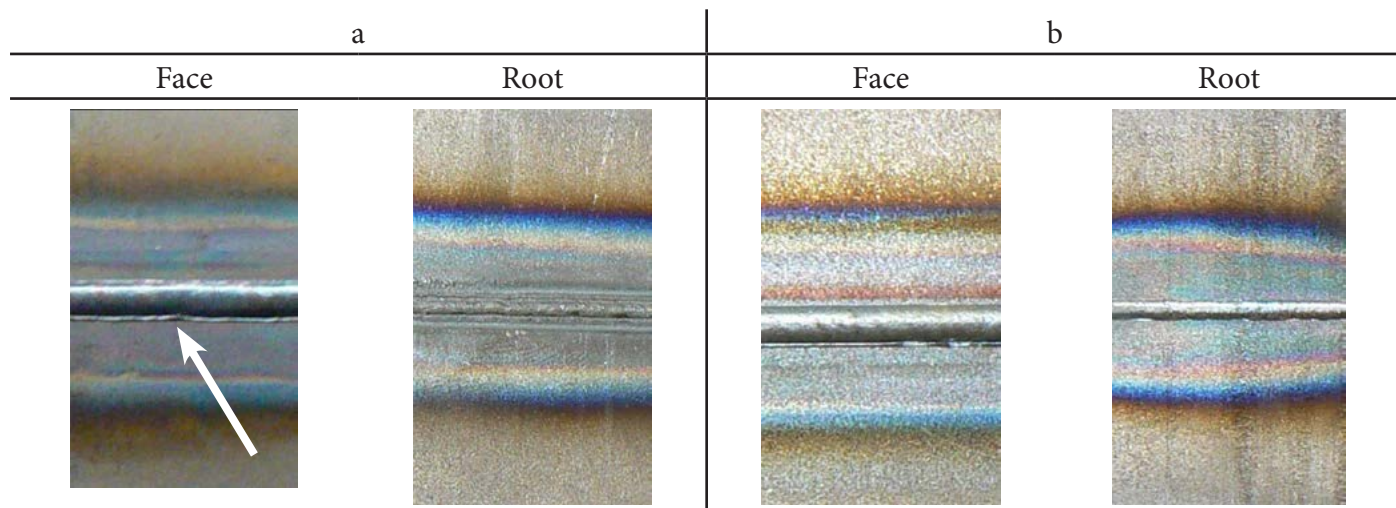


Fig. 3. Face and root of the weld in the plasma welded joint with the undercut area marked: a) $v_{sp}=22$ cm/min, linear energy $E = 0.48$ kJ/mm, b) $v_{sp}=33$ cm/min, linear energy $E = 0.32$ kJ/mm

Cross-sectional hardness tests of welded joints were performed using the Vickers hardness test according to PN-EN ISO 6507-1: 2007 and the load of a diamond pyramid amounting to 500 g. The tests were performed using a 401 MVD microhardness tester manufactured by Wilson Wolpert. The measurements started in the weld axis and were performed in both directions; the distance between measurement points amounted to 0.2 mm. The measurement line ran in the middle of the weld thickness. The cross-sectional hardness measurement results

are presented in Figure 7. Tensile tests of the joints made at linear energy $E = 0.48$ kJ/mm and 0.32 kJ/mm were performed on 5 specimens for each welded joint. Afterwards, the obtained test results were averaged. The tensile test results are presented in Table 2. Bend tests were performed on 4 specimens for each joint; two with the extension of the root and two with the extension of the face of the weld. The bend tests were performed using a bending mandrel having diameter $d=10$ mm; the bend angle amounted to 180° .

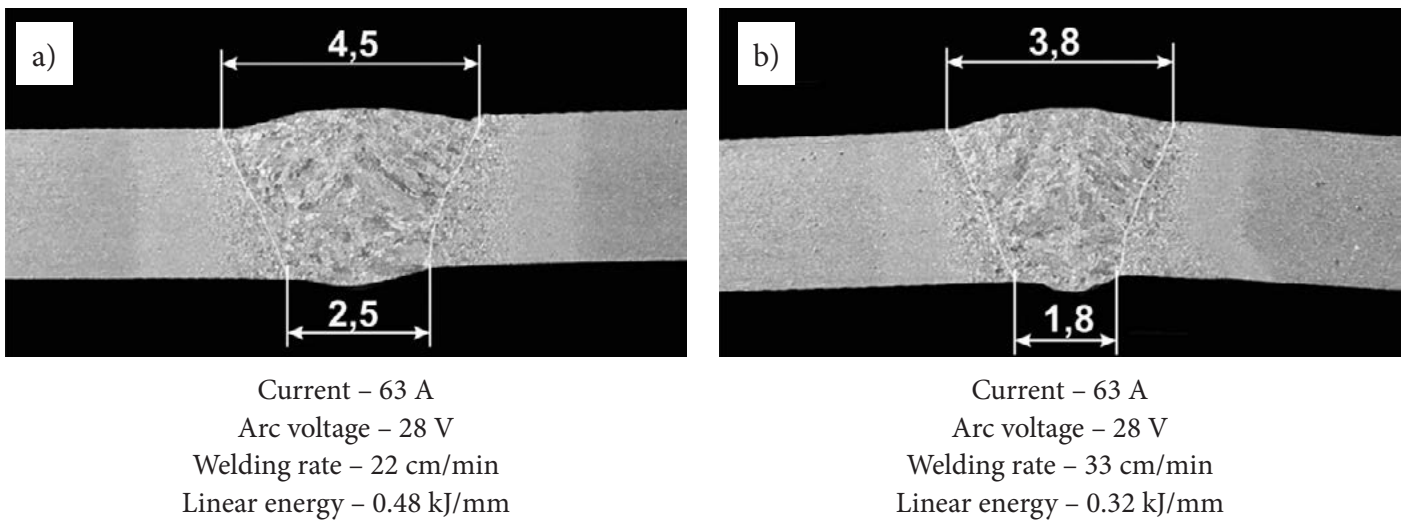


Fig. 4. Macrostructure of the plasma welded joints made of steel CPW 800 using various linear energy: $E = 0.48$ kJ/mm (a) and $E = 0.32$ kJ/mm (b). Etchant: Nital

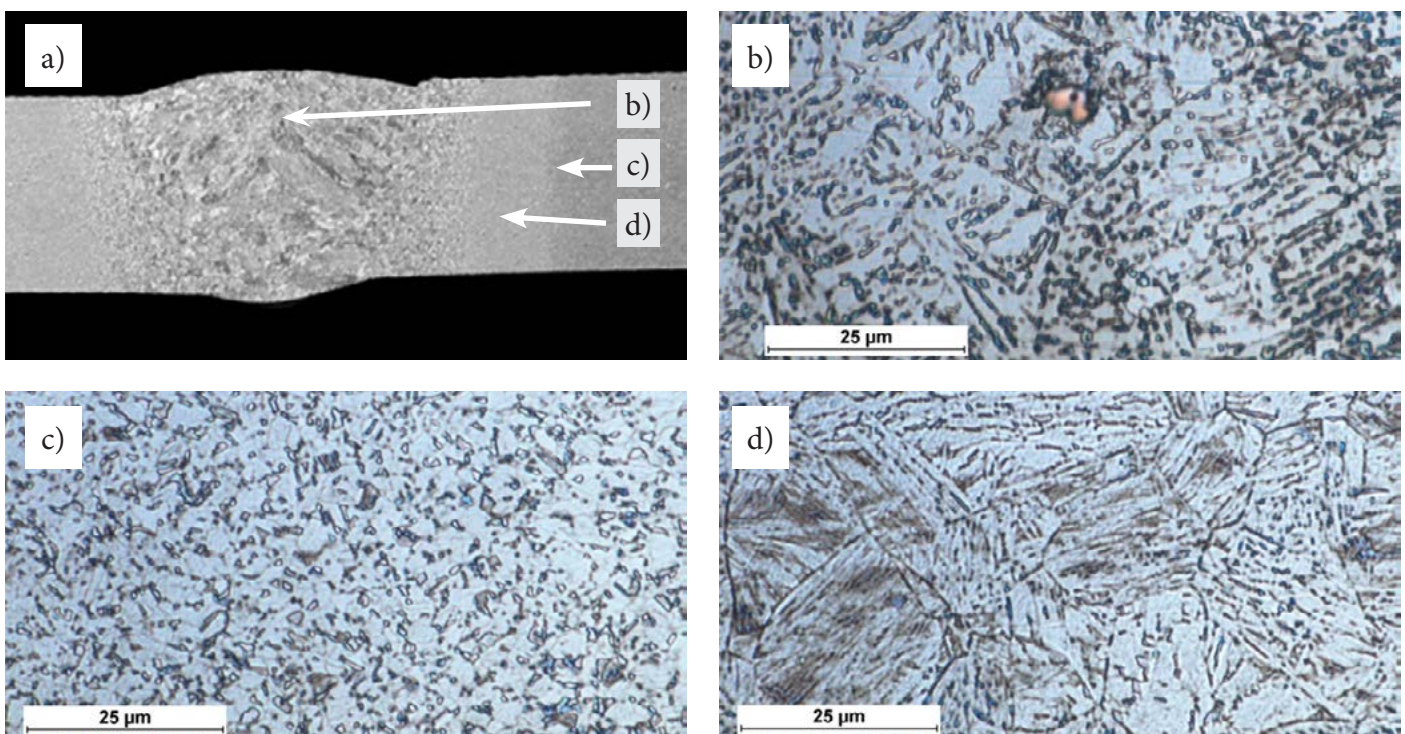


Fig. 5. Macro and microstructure of the plasma welded joint made at linear energy $E = 0.48$ kJ/mm: joint macrostructure (a), weld microstructure (b) and individual area of the HAZ (c, d). Etchant: Nital

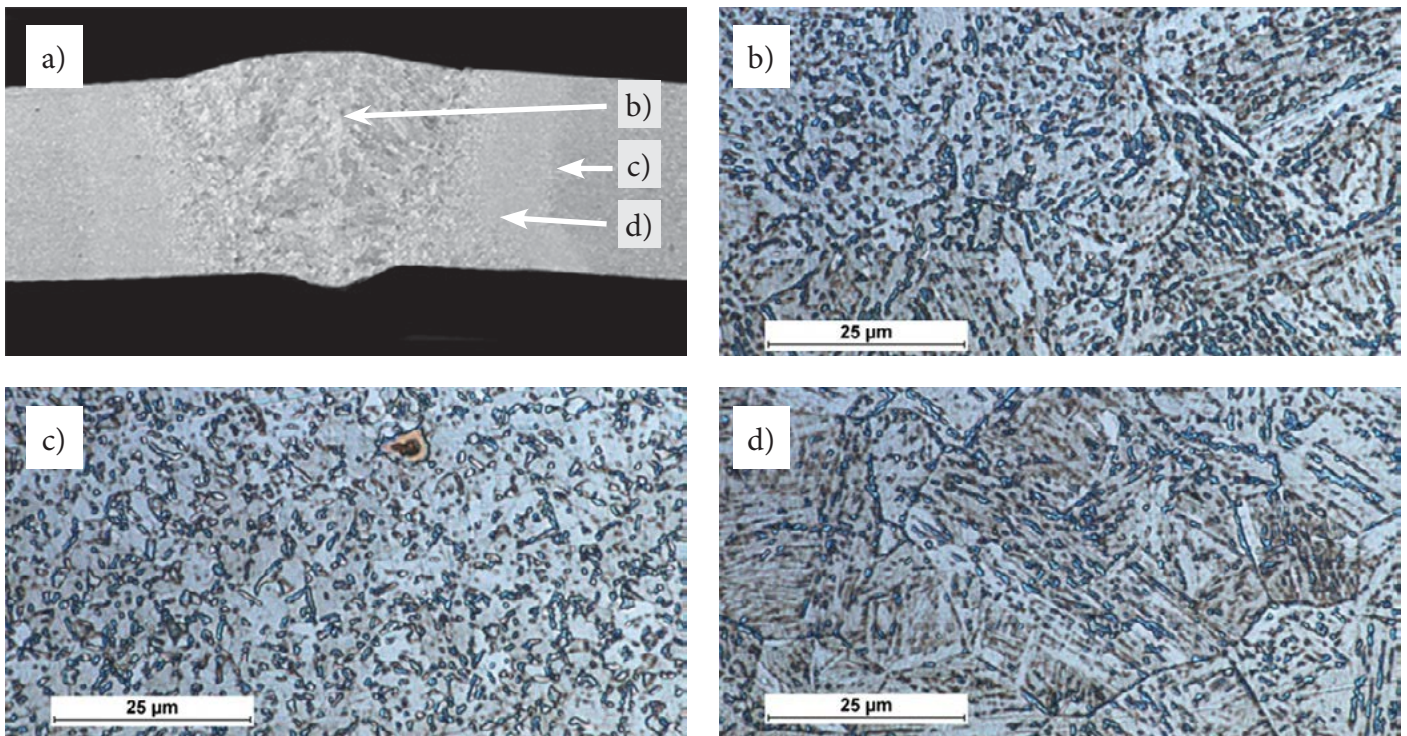


Fig. 6. Macro and microstructure of the plasma welded joint made at linear energy $E = 0.32$ kJ/mm: joint macrostructure (a), weld microstructure (b) and individual area of the HAZ (c, d). Etchant: Nital

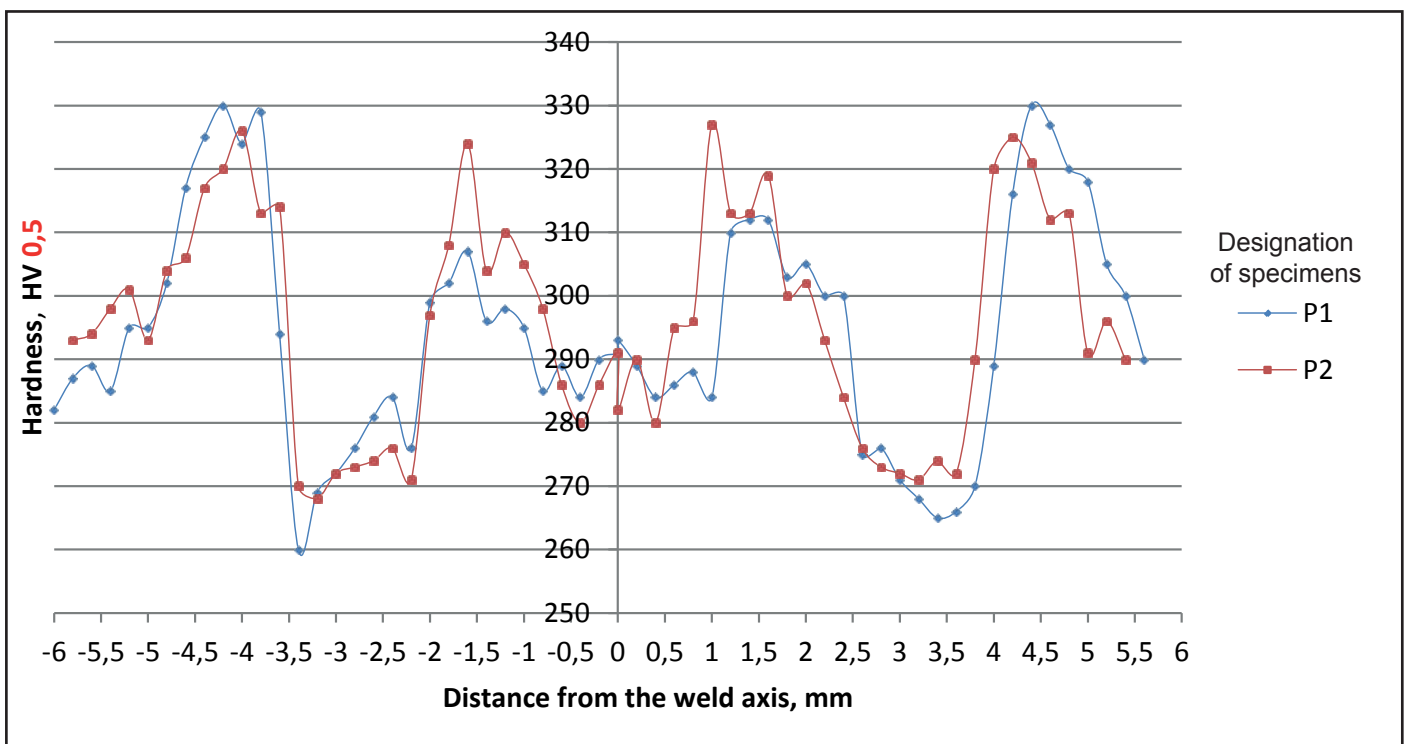


Fig. 7. Cross-sectional hardness distribution of the plasma welded joint made of steel CPW 800, P1 – made using linear energy $E = 0.48$ kJ/mm and P2 – made using linear energy $E = 0.32$ kJ/mm

Table 2. Results of tensile tests involving the test joints made at linear energy $E = 0.48$ kJ/cm and $E = 0.32$ kJ/mm

Tensile strength of the welded joints, MPa	
Test joint ($E = 0.48$ kJ/mm)	Test joint ($E = 0.32$ kJ/mm)
945; 899; 914; 901; 932; av. = 918	923; 935; 893; 895; 917; av. = 913

Summary of Test Results

The tests of the properties of plasma welded joints made of steel CPW800 involved visual tests, macro and microscopic metallographic tests, cross-sectional hardness measurements as well as tensile and bend tests.

The visual tests revealed that the specimen made at a welding rate of 22 cm/min and linear welding energy $E = 0.48$ kJ/mm, along the entire length of the joint on the weld face side, contained an undercut disqualifying the joint as meeting the requirements of quality level B according to PN-EN ISO 5817 (the joint satisfied the requirements of quality level C). The joint made at a welding rate of 33 cm/min did not contain any welding imperfections on the root and face side; the weld geometry was unchanged along the entire length of the joint.

The macroscopic metallographic tests confirmed the presence of an undercut in the joint made at a lower welding rate. In addition, the width of the weld on the face and root side amounted to 4.5 and 2.5 mm respectively and significantly exceeded the width of the face and root of the weld (3.9 mm and 1.8 mm respectively) made at a welding rate of 33 cm/min.

The microscopic metallographic tests revealed that the structure of the weld was composed of martensite (Fig. 5a and 6a). The HAZ on the weld side was composed of a mixture containing martensite and bainite (Fig. 5d and 6d). The transition area between the HAZ and the base material was characterised by a fine-grained mixture composed of bainite, ferrite and retained austenite (Fig. 5c and 6c). The increased content of fine-grained retained austenite in the transition area resulted from the partial enrichment of austenite in carbon within the range of intercritical temperatures (between A_{c1} and A_{c3}). In addition, significant precipitates (probably carbonitrides containing primarily Ti and a slight amount of Nb) on grain boundaries (Fig. 6d) were observed. The precise determination of the composition of precipitates requires

further tests involving X-ray or electron diffraction spectral analysis.

The hardness of the base material of steel CPW 800 was restricted within the range of 270 to 290 HV_{0.5}. The hardness tested on the cross-section was restricted within the range of 260 to 330 HV_{0.5}; the hardness of the weld itself did not exceed 300 HV_{0.5}. In the fusion line and in the area adjacent to it, the hardness increased to 300-315 HV_{0.5}. In the HAZ area adjacent to the fusion line, the hardness decreased to 260-280 HV_{0.5} and increased to approximately 330 HV_{0.5} in the HAZ. As regards the joint welded at linear energy $E=0.48$ kJ/mm, the hardness was slightly higher in the fusion line zone than in the joint made at linear welding energy $E=0.32$ kJ/mm. Small changes in the hardness on the cross-section could be attributed to structural changes and precipitation processes triggered by the welding thermal cycle.

Tensile tests revealed that in each case the tensile strength exceeded 890 MPa; the average of five tests performed for the joint welded at a linear energy of 0.48 kJ/mm and 0.32 kJ/mm amounted to 918 MPa and 913 MPa respectively. In each case, the specimens ruptured in the base material, far away (10 - 20 mm) from the welded joint. In turn, bend tests involving the tension of the weld face and root revealed the high plasticity of the joints; at a bend angle of 180°, the surface of welds and that of the HAZ were free from any scratches and cracks.

Conclusions

1. The conducted plasma welding technological tests confirmed the possibility of obtaining good quality welded joints of 2.5 mm thick sheets made of Complex Phase steel. The process of welding was characterised by high stability; the obtained welded joints revealed penetration across the entire thickness of the base material without cracks and porosity.
2. The welded joint made at a welding rate of 22 cm/min and linear energy $E=0.48$ kJ/mm contained an undercut. An increase in a weld-

ing rate to 33 cm/min (linear welding energy $E=0.32$ kJ/mm) without changing the remaining parameters eliminated undercuts when making a weld.

3. A dynamic thermal cycle of plasma welding results in the formation of a structure characterised by a high content of hard structural components, i.e. martensite and bainite, yet a limited content of carbon in steels makes the above named structural components only slightly supersaturated with carbon and, as regards welding, leads to a satisfactory hardness not exceeding 330 HV0.5.

4. The significant content of bainite in steel CPW 800 is responsible for the hardness of the base material being only by 15-20% lower than that of the joint, which ensures the relatively high uniformity of the mechanical properties of joints and base material.

5. The tensile strength of tested welded joints was between 893 MPa and 945 MPa; in each case, a specimen subjected to tension ruptured far away from the weld.

References

- [1] Adamczyk J., Grajcar A.: *Blachy samochodowe typu DP i TRIP walcowane metodą obróbki cieplno-mechanicznej*. Hutnik – Wiadomości Hutnicze, 2004, no. 7-8, pp. 305-309.
- [2] Kowielski S., Mikno Z., Pietras A.: *Zgrzewanie nowoczesnych stali o wysokiej wytrzymałości*. Biuletyn Instytutu Spawalnictwa, 2012, no. 3, pp. 5-14.
- [3] Rutkowski D., Ambroziak A.: *Effect of laser strengthening on the mechanical properties of car body steels presently used in automotive industry*. Biuletyn Instytutu Spawalnictwa, 2014, no. 5, pp. 49-57; http://bulletin.is.gliwice.pl/index.php?go=current&ebis=2014_05_06
- [4] Stano S.: *Spawanie laserowe blach o zróżnicowanej grubości przeznaczonych na półfabrykaty karoserii samochodowych typu tailored blanks*. Biuletyn Instytutu Spawalnictwa, 2005, no. 2, pp. 24-28.
- [5] Grajcar A., Różański M.: *Spawalność wysokowytrzymałych stali wielofazowych AHSS*. Przegląd Spawalnictwa, 2014, no. 3, pp. 22-31.
- [6] Grajcar A.: *Struktura stali C-Mn-Si-Al kształtowana z udziałem przemiany martenzytycznej indukowanej odkształceniem plastycznym*. Wydawnictwo Politechniki Śląskiej, Gliwice 2009.
- [7] Gould J.E., Khurana S.P., Li T.: *Predictions of microstructures when welding automotive advanced high-strength steels*. Welding Journal, 2006, no. 5, pp. 111-116.
- [8] Cretteur L., Koruk A.I., Tosal-Martinez L.: *Improvement of weldability of TRIP steels by use of in-situ pre- and post-heat treatments*. Steel Research, vol. 73, 2002, pp. 314-319.
- [9] Lisiecki A., Mańka J.: *Spawanie blach ze stali S420MC o podwyższonej granicy plastyczności laserem diodowym dużej mocy*. Biuletyn Instytutu Spawalnictwa, 2012, no. 3, pp. 67-71.
- [10] Gruszczak A., Griner S.: *Własności połączeń spawanych i zgrzewanych stali obrabianych termomechanicznie*. Przegląd Spawalnictwa, 2006, nos. 5-6, pp. 39-41.
- [11] Górka J.: *Własności i struktura złączy spawanych stali obrabianej termomechanicznie o wysokiej granicy plastyczności*. Wydawnictwo Politechniki Śląskiej, Gliwice 2013.